

1 **Confocal Raman Microscopy of Frozen Bread Dough**

2 Authors:

3 Julien Huen^{a,*}, Christian Weikusat^b, Maddalena Bayer-Giraldi^b, Ilka Weikusat^b, Linda Ringer^a,

4 Klaus Lösche^a

5 ^a ttz Bremerhaven, BILB-EIBT, Am Lunedeich 12, 27572 Bremerhaven, Germany

6 ^b Alfred Wegener Institute for Polar and Marine Research, Am Alten Hafen 26, 27570 Bremerhaven,

7 Germany

8 * Corresponding author. Tel.: +49 471 80934-241; fax: +49 471 80934-299.

9 E-mail addresses: jhuen@ttz-bremerhaven.de (Julien Huen), christian.weikusat@awi.de (Christian

10 Weikusat), maddalena.bayer@awi.de (Maddalena Bayer-Giraldi), ilka.weikusat@awi.de (Ilka

11 Weikusat), lring@ttz-bremerhaven.de (Linda Ringer), kloesche@ttz-bremerhaven.de (Klaus Lösche)

12 Keywords: Confocal Raman Microscopy, Frozen Bread Dough, Microstructure, Ice crystals.

13 **Abstract**

14 The use of freezing technology is well established in industrial and craft bakeries and is still gaining
15 importance. In order to optimize recipes and processes of frozen baked goods, it is essential to be
16 able to investigate the products' microstructure. Especially ice crystals and their interaction with the
17 other components of the frozen products are of interest. In this study, frozen wheat bread dough
18 was investigated by confocal Raman microscopy. The Raman spectra measured within the dough
19 were compared with spectra of the main components of frozen dough, i.e. ice, liquid water, starch,
20 gluten and yeast. In this way, the spatial distribution of the single components within the dough was
21 determined and corresponding images of the frozen dough microstructure were generated. On these
22 images, ice appears as a continuous network rather than as isolated crystals. We suggest that this
23 method may be appropriate for characterizing crystallization phenomena in frozen baked goods,
24 allowing to better understand the reasons for quality losses and to develop strategies for avoiding
25 such losses.

26 **1. Introduction**

27 As the bakery business is being concentrated and rationalized, increasing use is made of freezing
28 technology in production and distribution (Le Bail et al., 2012). Freezing allows a separation in time
29 and space of process operations that would traditionally be performed in one run and in one place.

30 In bread-making, freezing is used at several stages of production: for non-fermented or partly-
31 fermented dough, for partly or fully baked products (Le Bail et al., 2012). Depending on the
32 application, the products are kept frozen for a few hours or for several weeks or months. A large
33 variety of equipment, including shock-freezers, fermentation interrupters, climatic chambers, and
34 cold storage rooms are used for realizing the operations of freezing, cold storage and thawing.

35 Although the intention when using freezing is to keep the product in a steady state, in practice a
36 number of physical and chemical phenomena occur, affecting the quality of the final product in a
37 mostly negative way. Among these phenomena, the formation of ice crystals is believed to be of
38 primary importance for two main reasons (Berglund et al. 1991, Baier-Schenk et al. 2005a):

39 (1) Ice crystals are made of pure water which is being separated from the product matrix.
40 Cryoconcentration occurs in the liquid phase, which may influence the solubility of proteins and the
41 activity of enzymes. During storage, ice crystals grow due to recrystallization, especially in the pores,
42 thus further modifying the distribution of water in the product. (2) Ice crystals may mechanically
43 damage the dough components, especially the gluten network and the yeast cells, because the
44 freezing front exerts stress on the surrounding material. This effect is believed to be more
45 pronounced as the crystal size increases due to recrystallization.

46 In order to optimize the recipes and the production processes of frozen baked goods, it is essential to
47 be able to monitor the phenomena occurring in the products in the frozen state. Differential
48 scanning calorimetry (DSC) allows quantitative investigations of ice crystallization. For monitoring the
49 size and the distribution of the ice crystals as well as their mechanical interactions with the other
50 components of the dough, imaging techniques are required. So far, scanning electron microscopy in

51 the frozen state (cryo SEM, Zounis et al. 2002, Esselink et al., 2003, Baier-Schenk et al. 2005a) and
52 confocal laser scanning microscopy (CLSM, Baier-Schenk et al. 2005b) have been used for that
53 purpose. Cryo SEM has allowed demonstrating the growth of ice crystals within the pores over
54 storage time and CLSM to identify regions of preferential nucleation. However, in both techniques, a
55 difficulty is the limited possibility to unambiguously differentiate the ice crystals from the other
56 components of the dough. In cryo SEM, this differentiation is performed based on the regular shape
57 of the crystals – but this is only valid in the pores, where ice crystals can grow without spatial
58 constraints. In CLSM, changes in the reflection properties were attributed to ice crystal growth.
59 However, this method did not allow for generating precise images of the ice crystal structure. Due to
60 these limitations, little is known about the structure of the ice crystals that are entrapped in the
61 dough matrix, which yet represent the main part of the frozen water.

62 Raman spectroscopy belongs to the group of vibrational spectroscopies (Smith et al., 2005). It utilizes
63 the inelastic scattering of light photons on molecules or molecular groups, called Raman effect. If the
64 molecule (or group) has suitable vibrational modes, a photon can transfer a fraction of its energy to
65 the vibration (Stokes scattering). The positions of the Raman bands directly give the energy of the
66 detected vibrations. The ensemble of Raman active vibrations is characteristic for each compound
67 and can range from single bands to very complex multi-band spectra. Raman spectroscopy is a non-
68 destructive method requiring very little sample preparation and it is suitable for a wide range of
69 materials. If high-quality reference spectra are available, it is a very sensitive tool for phase
70 identification.

71 With the implementation of Raman spectroscopy in confocal microscopy in the late 1990s, it became
72 possible to use Raman data for microimaging purposes. Applications were developed in a variety of
73 scientific fields including mineralogy, petrography, polymer science, pharmaceutical research (Dieing
74 et al., 2011), biomedical diagnostics (Krafft et al., 2012) and glaciology (Weikusat et al., 2012). In
75 agricultural and food science and more specifically in cereal science, only little use has been made of
76 this technique so far. Piot et al. (2000, 2001, 2002) used confocal Raman microscopy for exploring

77 the spatial distribution of starch, gluten, arabinoxylan and ferulic acid in wheat grains. Recently,
78 Jääskeläinen et al. (2013) performed similar investigations with higher (sub- μm) spatial resolution on
79 barley and wheat grains.

80 Based on the fact that confocal Raman microscopy has shown to be suitable for characterising both
81 ice crystals and the main components of cereals, our objective was to develop a measurement
82 method appropriate for investigating the microstructure of frozen bread dough.

83 **2. Experimental**

84 **2.1. Raw materials and equipment**

85 The following ingredients were used in the experiments: Wheat flour type 550 (Roland Mühle,
86 Germany), compressed yeast (Frischhefe, Deutsche Hefewerke GmbH, Germany), and salt (Suprasel
87 fine, Suprasel, The Netherlands).

88 Raman measurements were performed on a WITec Alpha 300R microspectroscopy system equipped
89 with a frequency-doubled Nd:YAG laser ($\lambda = 532 \text{ nm}$), an UHTS300 Raman Spectrometer (grating: 600
90 grooves/mm, pixel resolution $<0.09 \text{ nm}$) with a Peltier-cooled DV401A-BV CCD detector (peak
91 quantum efficiency at $\sim 550 \text{ nm}$ and -60°C : $>95\%$) and a 50x LWD objective, operated in a cold
92 laboratory at -15°C at the Alfred-Wegener Institute. The laser power on the sample was $<30\text{mW}$.

93 **2.2. Assessment of Raman spectra of single dough components**

94 The Raman spectra of ice, liquid water, starch, gluten, and yeast were assessed using the following
95 procedure.

96 **2.2.1. Sample preparation**

97 A 3.5% (w/v) salt solution in bidistilled water was prepared. One droplet of this solution ($20 \mu\text{L}$) was
98 placed on a microscope slide, covered with a cover slip using a 2 mm spacer to standardize thickness,
99 and frozen at -20°C . In this way ice crystals and a liquid phase (cryoconcentrated salt solution) were

100 formed. The salt present in the liquid phase is expected to influence the Raman spectrum only to a
101 minimal extent, as its main component NaCl ($\geq 99,8$ % according to the supplier's specification) has
102 no molecular vibration.

103 Wheat flour was hydrated and separated into a starch suspension and a wet gluten piece using a
104 Glutomatic 2200 from Perten Instruments, Sweden. One droplet of the starch suspension was placed
105 on a microscope slide, covered with a cover slip using a 2 mm spacer and frozen at -20°C . The same
106 was done with a small portion of the wet gluten piece and of the compressed yeast block.

107 **2.2.2. Measurement**

108 The Raman spectrum of each of the samples representative for the individual dough components
109 was measured at 10 different points, with 20 accumulations of 1 s each per point, and the average
110 spectrum was calculated for each component.

111 **2.3. Dough sample preparation**

112 Three frozen dough samples were prepared at three different days in the following way: 50 g of
113 wheat flour, 28 g of bidistilled water, 1.5 g of compressed yeast and 1 g of salt were mixed and
114 kneaded to a dough in a Brabender Farinograph AT at 20°C . The mixing time was 2 minutes at 36 rpm
115 and the kneading time 4 min at 63 rpm. After kneading, the dough was allowed to rest for 15 min at
116 room temperature. Subsequently, a small piece (approx. 250 mg) of the inner part of the dough was
117 cut out, placed on a microscope slide, covered with a cover slip using a 2 mm spacer and frozen
118 at -20°C .

119 **2.4. Confocal Raman microscopy of frozen dough samples**

120 On the day following preparation, the samples were transferred to the microscopy laboratory
121 at -15°C . Before measurement, the samples were kept for at least one hour at -15°C to stabilize at
122 that temperature.

123 For each of the 3 frozen dough samples, an area of 100 x 100 μm was measured with a resolution of
124 200 x 200 points and an integration time of 1 s per point, resulting in a measurement time of approx.
125 12 hours.

126 **2.5. Confocal Raman microscopy: data processing and imaging**

127 The data from the area scans were processed in two different ways to produce images showing the
128 spatial distribution of the single dough components (ice, liquid water, starch, gluten and yeast).

129 In the first method, single Raman bands characteristic for each component were integrated.

130 Monochrome images were generated representing the intensity of the individual bands at each
131 measurement point. The spectral ranges of the chosen bands are given in Table 1 and are marked in
132 blue in Figure 1.

133 The second method considered the full Raman spectra instead of single bands. In that method, the
134 Raman spectrum measured at each point of the sample was assumed to be a linear combination of
135 the spectra of the single dough components. After performing a 3rd order polynomial background
136 subtraction on all spectra, a multiple linear regression was completed using the function *Basis*
137 *Analysis* of the WITec Project software (release 2.10, WITec GmbH, Ulm, Germany). The assessed
138 regression coefficients were used as indicators of the concentration of the individual dough
139 components, and corresponding monochrome images were generated. This method is well
140 established in confocal Raman microscopy and was used among others by Jääskeläinen et al. (2013).

141 The monochromatic images showing the distribution of the single components were combined to
142 colour images in which each colour represents one component. This allows visualizing the position
143 and distribution of the components relative to each other.

144 3. Results

145 3.1. Raman spectra of single dough components

146 The measured spectra of the single dough components are presented in Figure 1, and bands of
147 particular interest are listed in Table 1.

148 Ice is especially characterized by the OH stretching band with a maximum in the spectral range of
149 3080-3200 cm^{-1} , as described by Đuričković et al. (2011). This band was not found in the spectra of
150 the other dough components. The spectrum of liquid water is dominated by the OH stretching band
151 with a maximum in the range of 3300-3420 cm^{-1} , and also embodies the OH bending band (1580-
152 1640 cm^{-1}). Starch shows a series of bands, reflecting its molecular complexity. These bands were
153 already reported by Piot et al. (2000) and Fechner et al. (2005) and their assignment discussed by
154 these authors. The CH stretching band (2800-3050 cm^{-1}) and the OH stretching band are both
155 strongly represented. The narrow band in the range of 460-510 cm^{-1} , which is attributed to the
156 stretching vibration of the carbon network of starch, was not found in spectra of the other dough
157 components. The gluten spectrum shows a higher base signal, due to fluorescence, and a series of
158 bands that were described and which assignment was discussed by Piot et al. (2000). As in starch, the
159 CH stretching band is strongly represented. The band in the range of 1645-1690 cm^{-1} is attributable,
160 at least partly, to amide I (see “band position and assignment” in the discussion).

161 Yeast also shows a high base signal caused by fluorescence. The observed bands are in line with the
162 measurements of Rösch et al. (2006) with *Saccharomyces cerevisiae*. In the range of 1645-1690 cm^{-1} ,
163 yeast show a signal similar to gluten, yet with lower intensity. The band in the range of 740-766 cm^{-1} ,
164 which was assigned by the latter authors to tryptophan, appears to be specific for yeast in the
165 studied dough system in terms of intensity – gluten and to a lesser extent starch also have bands in
166 this spectral range, but they are weaker.

167 **3.2.Raman images of frozen dough**

168 The figures 2, 3 and 4 show the spatial distribution of the individual dough components within the
169 three samples, as determined by both data processing methods (band integration and multiple linear
170 regression). The distribution of liquid water, however, was determined only by multiple linear
171 regression, as the OH Raman bands of liquid water overlap with the OH bands of the starch and the
172 gluten spectra – in other words, liquid water has no specific single Raman band in the frozen dough
173 system. Multiple linear regression, on the other hand, failed to allow for a determination of the
174 distribution of yeast, as is discussed below. For each sample, a colour image showing the relative
175 spatial distribution of the single dough components was generated.

176 Both representations are complementary. The monochrome images give more details about the
177 structure of the single components. Due to the depth of field of a few μm , it gives some insights into
178 the 3-dimensional structure. Elements located a few μm above or below the focal plane are still
179 being detected but lead to a weaker signal, which is represented by a lower pixel brightness. The
180 colour images, on the other hand, show how the dough components are spatially organized relatively
181 to each other in the focal plane.

182 Starch appears on the pictures as large granules with a diameter of 20-25 μm and smaller granules
183 with a diameter of 2-5 μm . Gluten appears as fibrils organised around the starch granules, partly with
184 a spatial orientation as parallel strands. In the three samples studied, ice appears as a continuous
185 network rather than as single crystals. This network structure is better visible on the single-phase
186 than on the multi-phase pictures, due to the higher depth of field. Small ice blocks with a diameter of
187 1-10 μm , integrated in the ice network, are observed in some of the spaces between the starch
188 granules. Yeast cells appear on the picture as ellipsoids with a size of 4-5 μm , homogeneously
189 distributed within the samples. The yeast images also show a background noise, especially in the
190 gluten-rich regions. Liquid water appears to be present in the areas where no other phase is present.

191 **4. Discussion**

192 **Sample integrity**

193 In Raman microscopy, in order to obtain a detectable signal, a laser beam with high power density
194 needs to be applied in the focus area, which can result in heating and structural alteration. Especially
195 with frozen samples it is therefore essential to ascertain the integrity of the sample after the
196 measurements. In the case of the samples of the present study, routine microscopic inspection of the
197 Raman-mapped sample areas showed no signs of damage. Although it is not possible to measure
198 temperature within the sample during measurement, two observations suggest that temperature
199 was not significantly increased: (1) Ice and liquid water were found to be both strongly represented
200 in the investigated samples; this is consistent with the DSC measurements of frozen dough by Baier-
201 Schenk et al. (2005a), which show at -15°C about 50 % of the water are in the frozen state, whereas
202 the other 50 % are in the liquid form; (2) Repeated mappings of the same areas yielded identical
203 results; under the assumption of melting and recrystallization, a different distribution of ice would
204 have been observed.

205 **Band position and assignment**

206 The spectral bands used for imaging in the first method were chosen both by (1) comparing the
207 spectra of the single components on Figure 1 and searching for bands that are unique for each
208 component and (2) using knowledge from literature on band assignment. In the case the OH
209 stretching band of ice and the stretching vibration of the carbon network of starch, the high intensity
210 of the bands and their characteristic shape allows for a clear assignment. These bands are very
211 appropriate for identifying ice and starch in the frozen dough. The assignment of the amide I band is
212 more complicated due to the fact that the shape of the band and the position of its maximum
213 depends on the secondary and tertiary structure of the proteins (Tuma, 2005). A further difficulty lies
214 in the proximity of other bands. Finally, fluorescence, which is dependent on the excitation
215 wavelength, overlaps with the Raman signal. For these reasons, there is no certitude that the spectral

216 range selected (1645-1690 cm^{-1}) corresponds exclusively to amide I in gluten. In addition, it must be
217 noted that amide I can only be seen as an imperfect indicator of gluten in the frozen dough system,
218 as amide I signal is also expected to arise from non-gluten wheat protein and from yeast protein.

219 The use of the band 740-766 cm^{-1} for yeast identification in the dough must be considered as an
220 empirical approach. It is unclear whether the signal measured in this range is solely attributable to
221 the ring breathing vibration of tryptophan, nor whether tryptophan can be considered as a reliable
222 indicator or yeast in the dough system.

223 **Unambiguous identification and imaging of the single dough components**

224 As discussed above, starch and ice have good single band indicators in the frozen dough system, and
225 it is not surprising that for these components both data processing methods lead to similar pictures.

226 The pictures generated by multiple linear regression show less noise and are therefore sharper,
227 probably due to the fact that they are based on a broader data basis. In the case of gluten, a good
228 match between the pictures obtained from both data processing methods is observed as well.

229 The identification and imaging of yeast has a lower level of confidence, due to the limitations
230 described above. The noise observed on the images can be explained by the fact that gluten and
231 starch also have weak bands in the chosen spectral range. Imaging of yeast using multiple linear
232 regression was not successful, as the generated images were obviously wrong (no cell shape); this is
233 probably due to the overlap of the yeast signals with signals from the other dough components in
234 most spectral areas, as well as to the low abundance of yeast in the system.

235 Liquid water can be identified only by multiple linear regression, due to the overlap with the OH
236 bands of the other components.

237 **Spatial distribution of the single dough components**

238 The observed spatial distribution of starch, gluten and yeast is consistent with data from literature. A
239 bimodal size distribution of starch granules in wheat flour was reported by numerous authors like

240 Stoddard et al. (1999). The observed relative distribution of starch and gluten, with gluten fibrils
241 organised as a network around the starch granules, is consistent with observations made by other
242 techniques like scanning electron microscopy (Yi et al., 2009), confocal scanning laser microscopy and
243 epifluorescence light microscopy (Peighambardoust et al., 2010). The observed size and shape of the
244 yeast cells is in line with literature data (Smith et al., 2000).

245 The most interesting, and really novel aspect, is the distribution of ice. The structure of ice as a
246 continuous phase (crystal network) within the frozen dough has not, to our knowledge, been
247 reported elsewhere so far. This continuous structure may be of importance for understanding
248 damage to the other dough components, especially to gluten which also has a network structure –
249 meaning that in the frozen state, the gluten network and the ice crystal network coexist and are
250 embedded in one another.

251 **5. Conclusions**

252 In our investigations, confocal Raman microscopy allowed a reliable identification and imaging of
253 starch, ice and gluten; yeast and liquid water were identified with a lower degree of confidence. The
254 method is non-destructive and does not require any staining.

255 The unambiguous identification of ice based on its specific Raman spectrum (specific OH stretching
256 band) allows visualising the structure of ice within the frozen dough matrix. The structure of ice as a
257 network rather than isolated crystals represents a new finding that helps understanding the
258 interactions between the dough components in the frozen state.

259 We suggest that the technique described in this paper may be useful to study the influence of
260 different freezing and storage conditions, of different storage times, and of specific ingredients such
261 as ice structuring proteins, on the ice network structure in frozen dough. Such investigations may be
262 conducted either on a model system like in this study (dough frozen on a microscope slide), or on
263 microtome sections of real-life frozen products.

264 The technique in itself may be refined in terms of spatial resolution by the use of an objective with a
265 higher magnification and in terms of measurement speed by the use of a more sensitive
266 spectrometer. The use of a different excitation wavelength could help reducing fluorescence. More
267 detailed Raman spectroscopic studies of the single components of the dough, especially starch and
268 gluten, may allow differentiating between sub-components such as amylose, amylopectin, gliadin
269 and glutenin, ultimately leading to more detailed images.

270 Numerous further applications of cryo Raman microscopy are conceivable with other kinds of frozen
271 foods or frozen biological samples.

272 **6. Acknowledgements**

273 This research project was supported by the German Ministry of Economics and Technology (via AiF)
274 and the FEI (Forschungskreis der Ernährungsindustrie e.V., Bonn). Project AiF 17181 N.

275 Access to the cryo Raman microscope was provided by the Young Investigator Group VH-NG-802 of
276 the Helmholtz Association.

277 **7. References**

278 Baier-Schenk, A., Handschin, S., Conde-Petit, B., 2005a. Ice in prefermented frozen bread dough – an
279 investigation based on calorimetry and microscopy. *Cereal Chemistry* 82, 251-255.

280 Baier-Schenk, A., Handschin, S., von Schönau, M., Bittermann, A.G., Bächli, T., Conde-Petit, B., 2005b.
281 In situ observation of the freezing process in wheat dough by confocal laser scanning microscopy
282 (CLSM): formation of ice and changes in the gluten network. *Journal of Cereal Science* 42, 255-260.

283 Berglund, P.T., Shelton, D.R., Freeman, T.P., 1991. Frozen bread dough ultrastructure as affected by
284 duration of frozen storage and freeze-thaw cycles. *Cereal Chemistry* 68, 105-107.

285 Dieing, T., Hollricher, O., Toporski, J., 2011. *Confocal raman microscopy*. Springer, Heidelberg.

286 Đuričković, I., Claverie, R., Bourson, P., Marchetti, M., Chassot, J.M. and Fontana, M.D., 2011, Water-
287 ice phase transition probed by Raman spectroscopy. *Journal of Raman Spectroscopy* 42, 1408–1412.

288 Esselink, E. F. J., van Aalst, H., Maliepaard, M., van Duynhoven, J. P. M., 2003, Long-Term Storage
289 Effect in Frozen Dough by Spectroscopy and Microscopy. *Cereal Chemistry* 80, 396-403.

290 Fechner, P.M., Wartewig, S., Kiesow, A., Heilmann, A., Kleinebudde, P., Neubert, R.H.H., 2005.
291 Influence of water on molecular and morphological structure of various starches and starch
292 derivatives. *Starch/Stärke* 57, 605-615.

293 Jääskeläinen, A.S., Holopainen-Mantila, U., Tamminen, T., Vuorinen, T. , 2013. Endosperm and
294 aleurone cell structure in barley and wheat as studied by optical and Raman microscopy. *Journal of*
295 *Cereal Science* 57, 543-550.

296 Krafft, C., Dietzek, B., Schmitt, M., Popp, J., 2012. Raman and coherent anti-Stokes Raman scattering
297 microspectroscopy for biomedical applications. *Journal of Biomedical Optics* 17, 040801.

298 Le Bail, A., Zia, C., Giannou, V., 2012. Quality and safety of frozen bakery products. In: Sun, D.W. (Ed.),
299 *Handbook of frozen food processing and packaging*, Second edition. CRC Press, Boca Raton, pp. 501-
300 528.

301 Piot, O., Autran, J.C., Manfait, M., 2000. Spatial distribution of protein and phenolic constituents in
302 wheat grain as probed by confocal microspectroscopy. *Journal of Cereal Science* 32, 57-71.

303 Piot, O., Autran, J.C., Manfait, M., 2001. Investigation by Confocal Raman Microspectroscopy of the
304 Molecular Factors Responsible for Grain Cohesion in the *Triticum aestivum* Bread Wheat. Role of the
305 Cell Walls in the Starchy Endosperm. *Journal of Cereal Science* 34, 191-205.

306 Piot, O., Autran, J.C., Manfait, M., 2002. Assessment of cereal quality by micro-Raman analysis of the
307 grain molecular composition. *Applied Spectroscopy* 56, 1132-1138.

308 Rösch, P., Harz, M., Peschke K.-D., Ronneberg O., Burkhardt H., Popp, J., 2006. Identification of Single
309 Eucaryotic Cells with Micro-Raman Spectroscopy. *Biopolymers* 82, 312-316.

310 Smith, A. E., Zhang, Z., Thomas, C. R., Moxham, K. E., Middelberg, A. P., 2000. The mechanical
311 properties of *Saccharomyces cerevisiae*. *Proceedings of the National Academy of Sciences* 97, 9871-
312 9874.

313 Smith, E., Dent, G., 2005. *Modern Raman spectroscopy: a practical approach*. Wiley, Chichester.

314 Stoddard, F. L., 1999. Survey of starch particle-size distribution in wheat and related species. *Cereal*
315 *Chemistry*, 76, 145-149.

316 Tuma, R., 2005. Raman spectroscopy of proteins: from peptides to large assemblies. *Journal of*
317 *Raman Spectroscopy* 36, 307-319.

318 Thygesen, L.G., Løkke, M.M., Micklander, E., Engelsen, S.B., 2013. Vibrational microspectroscopy of
319 food. Raman vs. FT-IR. *Trends in Food Science and Technology* 14, 50–57.

320 Weikusat, C., Freitag, J., Kipfstuhl, S., 2012. Raman spectroscopy of gaseous inclusions in EDML ice
321 core: first results – microbubbles. *Journal of Glaciology* 58, 761-766.

322 Yang, D., Ying, Y., 2011. Applications of Raman spectroscopy in agricultural products and food
323 analysis: A review. *Applied Spectroscopy Reviews* 46, 539-560.

324 Yi, J., Kerr, W.L., 2009. Combined effects of freezing rate, storage temperature and time on bread
325 dough and baking properties. *LWT - Food Science and Technology* 42, 1474-1483.

326 Zhao, Y., Ma, C.Y., Yuen, S.N., Phillips, D.L., 2004. Study of Acetylated Food Proteins by Raman
327 Spectroscopy. *Journal of Food Science*, 69, 206-213.

328 Zounis, S., Quail, K.J., Wootton, M., Dickson, M.R., 2002. Effect of Final Dough Temperature on the
329 Microstructure of Frozen Bread Dough. *Journal of Cereal Science* 36, 135-146.

330 8. Tables

331 Table 1: Spectral ranges selected as characteristic for the single dough components. The references
332 cited provide a detailed discussion of the Raman spectra and of the band assignment for the
333 individual dough components.

Dough component	Spectral range (cm ⁻¹)	Band assignment	Reference
Ice	3080-3200	OH stretching band	Đuričković et al., 2011
Starch	460-510	Stretching vibration of the carbon network	Piot et al., 2000 Fechner et al., 2005
Gluten	1645-1690	Amide I (partly)	Piot et al., 2000
Yeast	740-766	Ring breathing vibration of tryptophan (possibly)	Rösch et al., 2006

334 9. Figure Captions

335 Figure 1: Raman spectra of single dough components: ice, liquid water, starch, gluten and yeast. The
336 spectral ranges used for band integration imaging are marked in blue.

337 Figure 2: First sample: Distribution of the dough components according to both data processing
338 methods (left: band integration; right: multiple regression). Colour code of the bottom image: starch
339 = red, gluten = yellow, ice = white, liquid water = green.

340 Figure 3: Second sample: Distribution of the dough components according to both data processing
341 methods. Colour code of the bottom image: starch = red, gluten = yellow, ice = white, liquid water =
342 green.

343 Figure 4: Third sample: Distribution of the dough components according to both data processing
344 methods. Colour code of the bottom image: starch = red, gluten = yellow, ice = white, liquid water =
345 green.

10. Figures

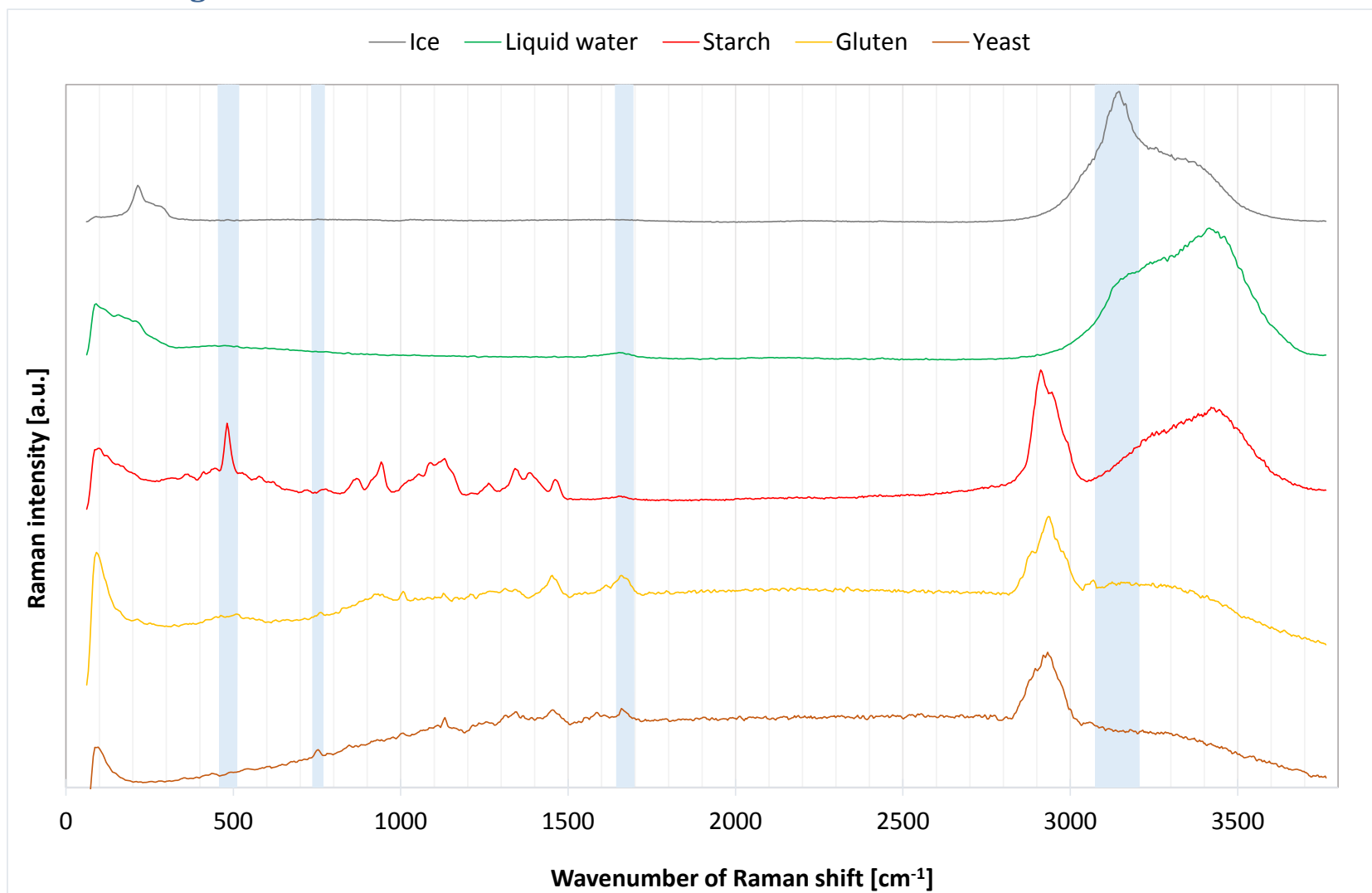


Figure 1

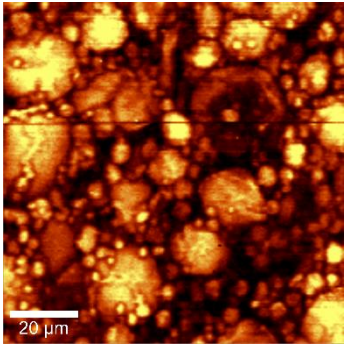
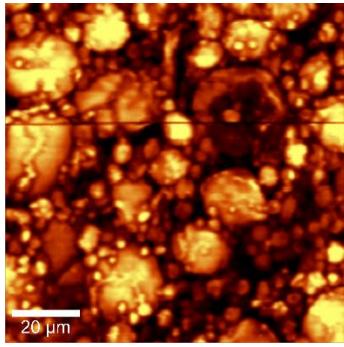
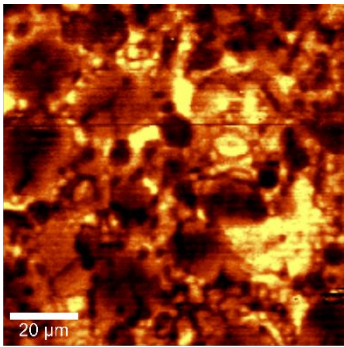
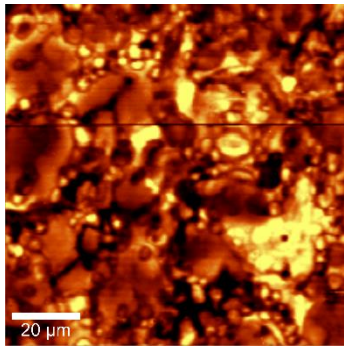
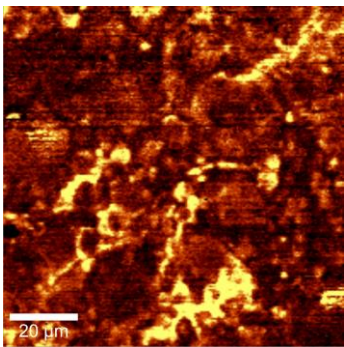
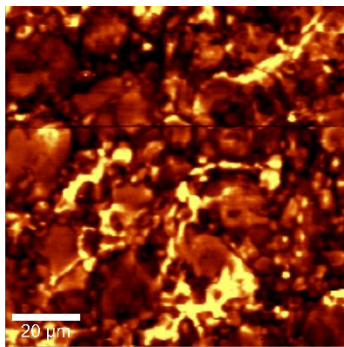
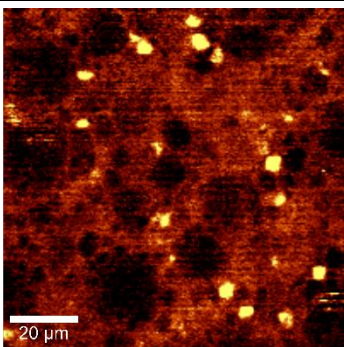
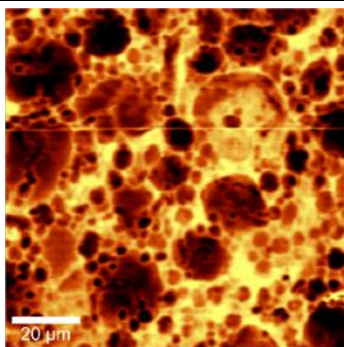
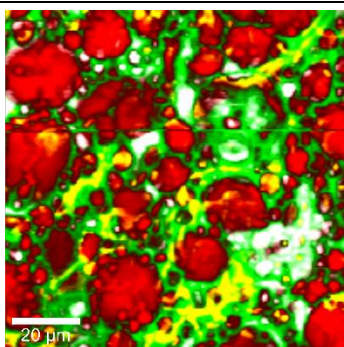
	Band integration		Multiple regression
Starch		Starch	
Ice		Ice	
Gluten		Gluten	
Yeast		Liquid water	
		Combined image	

Figure 2

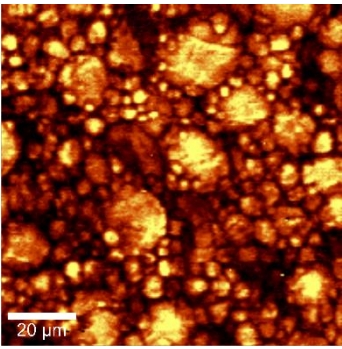
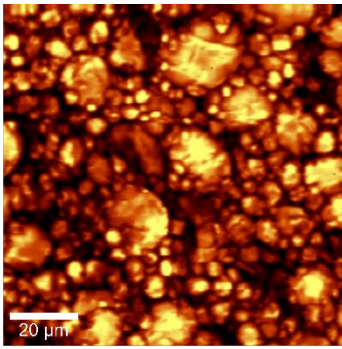
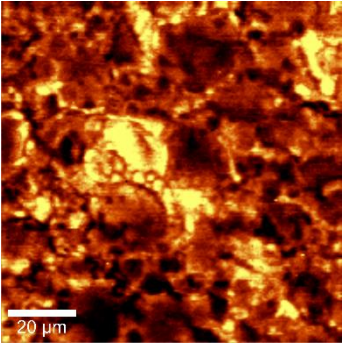
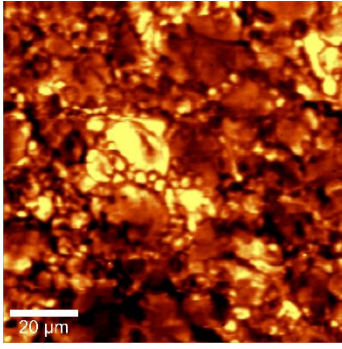
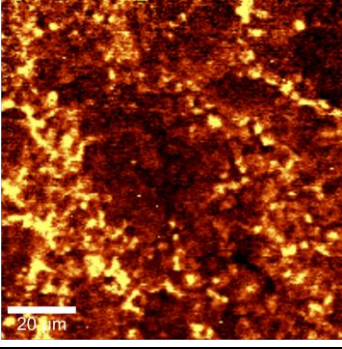
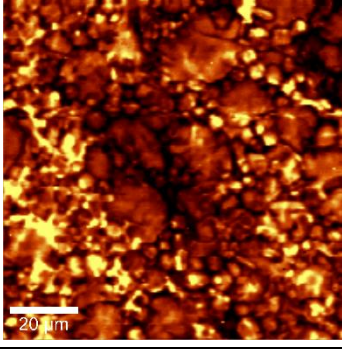
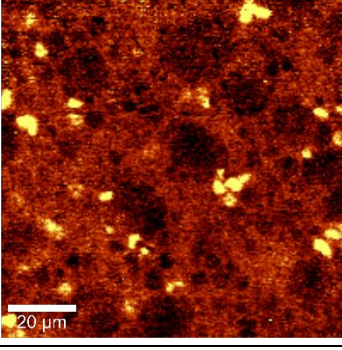
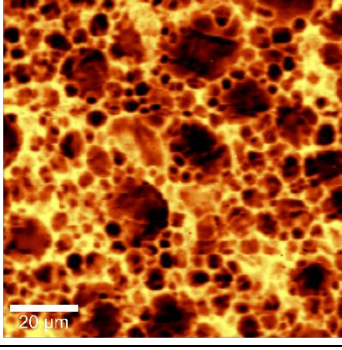
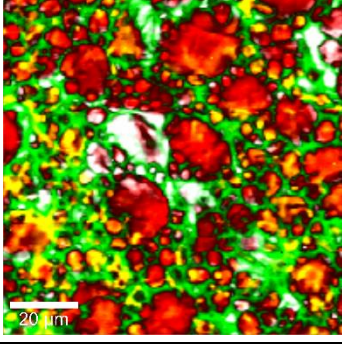
	Band integration		Multiple regression
Starch		Starch	
Ice		Ice	
Gluten		Gluten	
Yeast		Liquid water	
		Combined image	

Figure 3

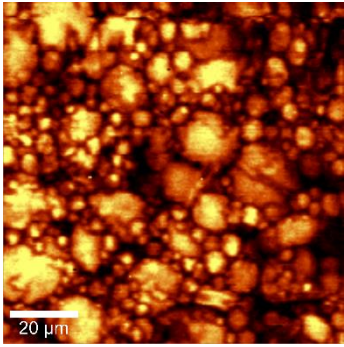
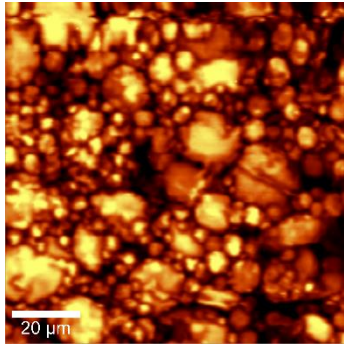
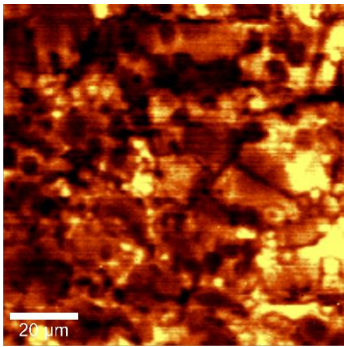
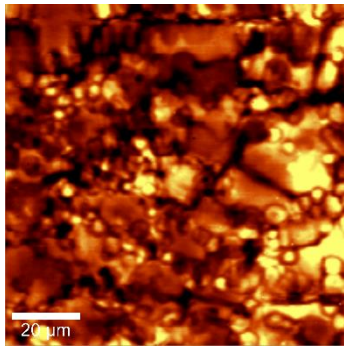
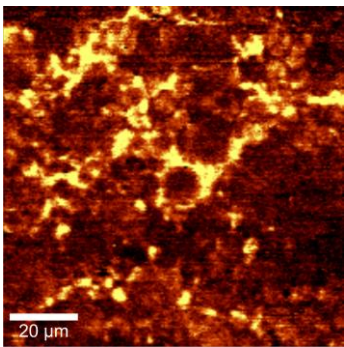
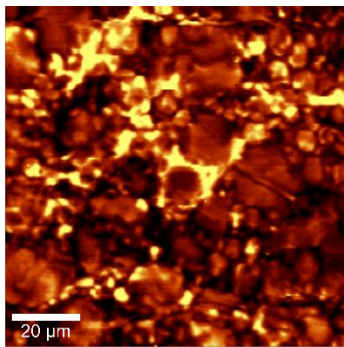
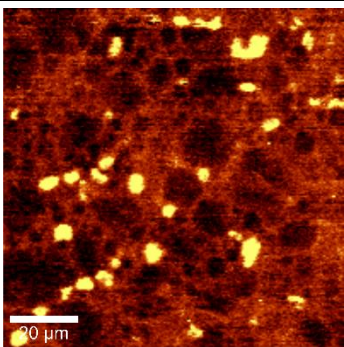
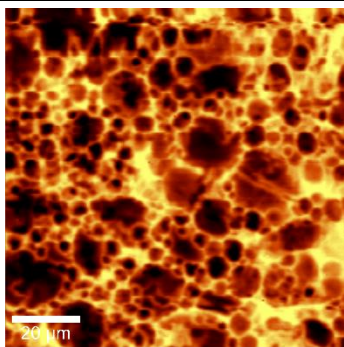
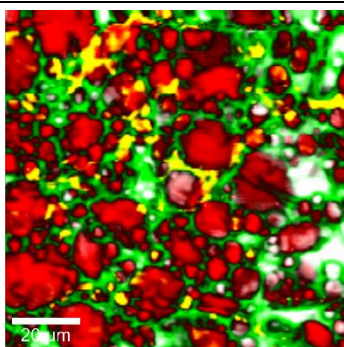
	Band integration		Multiple regression
Starch		Starch	
Ice		Ice	
Gluten		Gluten	
Yeast		Liquid water	
		Combined image	

Figure 4